Solvent Isotopic Effects on a Surfactant Headgroup at the Air-Liquid Interface

Uvinduni I. Premadasa,[a] *Negar Moradighadi,*[b] *Kondalarao Kotturi,*[a] *Jeeranan Nonkumwong,*[a,c] *Md. Rubel Khan,*[a] *Marc Singer,*[b] *Eric Masson,*[*,a] *and Katherine L. A. Cimatu*[*,a]

[a]Department of Chemistry and Biochemistry, Ohio University, 100 University Terrace, 136 Clippinger Laboratories, Athens, Ohio 45701-2979, United States

[b]Institute for Corrosion and Multiphase Technology, Ohio University's Research and Enterprise Park, 342 West State Street, Athens, Ohio 45701, United States

[c]Department of Chemistry, Faculty of Science, Chiang Mai University, Chiang Mai 50200, Thailand

ABSTRACT

The geometry, arrangement, and orientation of a quaternary ammonium surfactant flanked by two methyl groups, a benzyl head, and an octyl tail, were assessed at the air-water and air-deuterium oxide (D_2O) interfaces using sum frequency generation vibrational spectroscopy (SFG). Remarkably, symmetric and asymmetric N-CH_3 stretches (at ~2979 and ~3045 cm^{-1}, respectively, in the SSP polarization combination) were visible in water but were negligible in deuterium oxide. We concluded that D_2O addition triggers the average reorientation of the dimethyl amino units parallel to the interface, and possibly changes the overall conformation of the surfactant. A reduced number of gauche defects in the surfactant octyl chain is also observed in D_2O. Tilt angles for the octyl chain (1.0 – 10.8º) are consistent with an ordered monolayer at the air-liquid interface.

INTRODUCTION

Solvent isotopic effects, i.e., differences in physical and chemical properties of solutes observed upon replacing hydrogen atoms with deuterium in a solvent, have been evaluated in systems such as surfactants,[1] lipid bilayers, and polymers in water and deuterium oxide (D_2O).[2-4] Even though many properties such as surface tension,[5-6] refractive indices,[7] molar volume, and polarizability are similar for H_2O and D_2O,[8] bond strengths and intermolecular interactions still differ from each other. D_2O tends to form stronger hydrogen bonds compared to H_2O and therefore has a higher density, viscosity, and boiling point.[7] Isotopic substitution of water results in shifts in critical points and phase boundaries of surfactant mixtures, which affect the formation of self-assembled aggregates.[1]

In this study, we assess solvent isotopic effects on the interfacial conformation of a surfactant at the air-water interface, using sum frequency generation vibrational spectroscopy (SFG).

Recent studies involving surfactants have focused on water interfacial structure[9] or the influence of broad O-H and O-D stretch bands on the C-H stretching modes;[10] yet very few assess solvent effects on the structure of the interfacial surfactant itself.[9, 11] Here, we chose quaternary ammonium cation **1** (see supporting information section for its preparation),[12] as it belongs to the important class of "Quat" cationic surfactants used as corrosion inhibitors, especially for carbon steel in acidic media.[13-14]

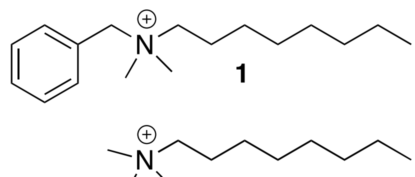

1

2

Surfactants are amphiphilic molecules consisting of a hydrophilic head and a hydrophobic tail.[3] When a surfactant is adsorbed at the air-water interface, the hydrophilic head group is directed into the water layer, and the hydrophobic tail is pointing towards the air. Moreover, charged head groups generate an electrostatic field in the double-layer region of the interface and affect the orientation and the number of water molecules present in this layer.[9,15] We are thus seeking to assess the impact of solvent isotopic substitution on the surfactant conformation, orientation, and solvation at the air-water interface using SFG spectroscopy.

The theoretical background of the SFG technique, as well as a detailed description of the experimental setup, are presented in earlier publications from our group.[16-17] In a typical experiment, the visible and mid-infrared (IR) beams are overlapped temporally and spatially on the sample surface; the generated SFG beam from the sum of the two incident beam frequencies is then collected and detected. SFG spectra contain information about the conformation of interfacial molecules and the orientation of selected species both at the surface and interface using various polarization combinations.

EXPERIMENTAL SECTION

The detailed description of the synthesis of Quat 1, sample preparation, and SFG experimental methods are provided in the supporting information. Solutions of surfactant **1** (60 mL, 8.0 mM) were prepared in H_2O, D_2O, and in a 1:1 (v/v) H_2O/D_2O mixture. In the latter case, as the equilibrium constant for the exchange between H_2O, D_2O, and 2 HOD is 3.86,[18] the H_2O/HOD/D_2O ratio is approximately 1:2:1. The SFG spectra were recorded with SSP and PPP polarization combinations in the CH regions; S and P refer to the beam perpendicular and parallel, respectively, to the plane of incidence. The polarized beams are listed in the order of decreasing energy; SSP stands for SFG (S), visible (S), and mid-IR (P) beams, respectively.[16]

RESULTS AND DISCUSSION

Quat **1** generates SFG signals from the vibrational modes of (1) the terminal methyl group of the octyl chain, (2) the methylene units, (3) the ammonium methyl groups, and (4) the benzyl unit. Figures 1a and 1b show, respectively, the SSP- and PPP-polarized fitted SFG spectra of Quat **1** in H_2O (top panel), in a 1:1 mixture of H_2O and D_2O (middle panel) and in D_2O (bottom panel); the simplified version of the fitting equation is presented in the SI section. In the SSP polarized spectra (see Figure 1a), the two peaks highlighted in green are assigned to the methylene symmetric stretch (CH_2 SS)[19-20] at ~2850 cm^{-1} and to the terminal methyl symmetric stretch (CH_3 SS)[19-22] at ~2875 cm^{-1}. All peak positions were taken from the fitting results (see Tables S1-S3). The two peaks highlighted in blue are assigned to the methylene asymmetric stretches (CH_2 AS) at ~2915 cm^{-1} and to the methyl Fermi resonance (CH_3 FR)[19-20, 22-23] at ~2930 cm^{-1}. The CH_3 FR signal can be fully described from the CH_3 SS split caused by the FR interaction with the methyl bending modes.[24] Ammonium methyl symmetric stretches (N-CH_3 SS)[25-27] at ~2979 cm^{-1}, and asymmetric stretches (N-CH_3 AS)[25-27] at ~3045 cm^{-1} are highlighted in orange and yellow, respectively. However, since the vibrational band at ~3045 cm^{-1} is broad , the peak can be a combination of both N-CH_3 AS and aromatic CH stretches.[28-30] The detection of the aromatic CH stretches benefits from the average position of the phenyl ring of the benzyl group when it is close to being positioned perpendicular to the surface plane.[29]

In the PPP polarized spectra (see Figure 1b), the highlighted regions from left to right are assigned to the methylene Fermi related mode (CH_2 FR)[19] at ~2850 cm^{-1}, terminal methyl symmetric stretches (CH_3 SS) at ~2885 cm^{-1}, methylene asymmetric stretches (CH_2 AS) at ~2920 cm^{-1}, and methyl asymmetric stretches (CH_3 AS)[20, 23] at ~2960 cm^{-1}. The CH_3 SS mode is shifted by ~10 cm^{-1} from SSP to PPP polarization combination due to the Fermi resonance interaction experienced by the methyl group with the overtone of the methyl bending vibrational mode.[24, 31-32] In addition, some vibrational modes from the head group are not visible in the PPP polarized spectra. This could be due to an intrinsically weak SFG signal caused by random orientation, or by an orientation change of the head group in the laboratory frame.[27] However, the Davies group recently reported[33] the SFG spectra of CTAB with a deuterated alkyl chain in water medium, and observed the N-CH_3 AS positioned at ~3025 cm^{-1} in both H_2O and D_2O at PPP polarization combination. Therefore, we carried out an additional experiment to support our results on the non-observation of the signature band of the N-CH_3 AS, and to determine the factor that can influence the observation of headgroup vibrational modes at PPP polarization combination. We recorded the spectrum of CTAB (0.10 mM in water) at 3000 cm^{-1} IR wave center, in both SSP and PPP polarization combinations (Figure S2). We did not observe the vibrational modes arising from the headgroup at PPP polarization combination, especially N-CH_3 AS (Figure S2 (b)). This observation is similar to that reported by Evan and coworkers with CTAB in water medium.[27] One possibility could be the differences in the experimental approach.

The Davies group used a 4.2 mM CTAB solution in $CHCl_3$, which was spread on water using a Teflon trough and had the ability to compress the monolayers, whereas the Evan group used a range of bulk concentrations from 50 μM to 2.0 mM in water. Our bulk concentration was ~0.10 mM CTAB; the aqueous solution was placed in a clean petri dish, and the experiment was carried out under N_2. Our conditions are thus rather similar to the ones used by Evan and coworkers, with a similar outcome.

Quat 1 Headgroup. While PPP polarized spectral profiles are not significantly solvent-dependent, important variations in the SSP polarized spectra are observed when H_2O is replaced with D_2O. In H_2O, the head group N-CH_3 SS, N-CH_3 AS, and aromatic CH stretch modes are visible, whereas in D_2O the signals are absent or negligible.

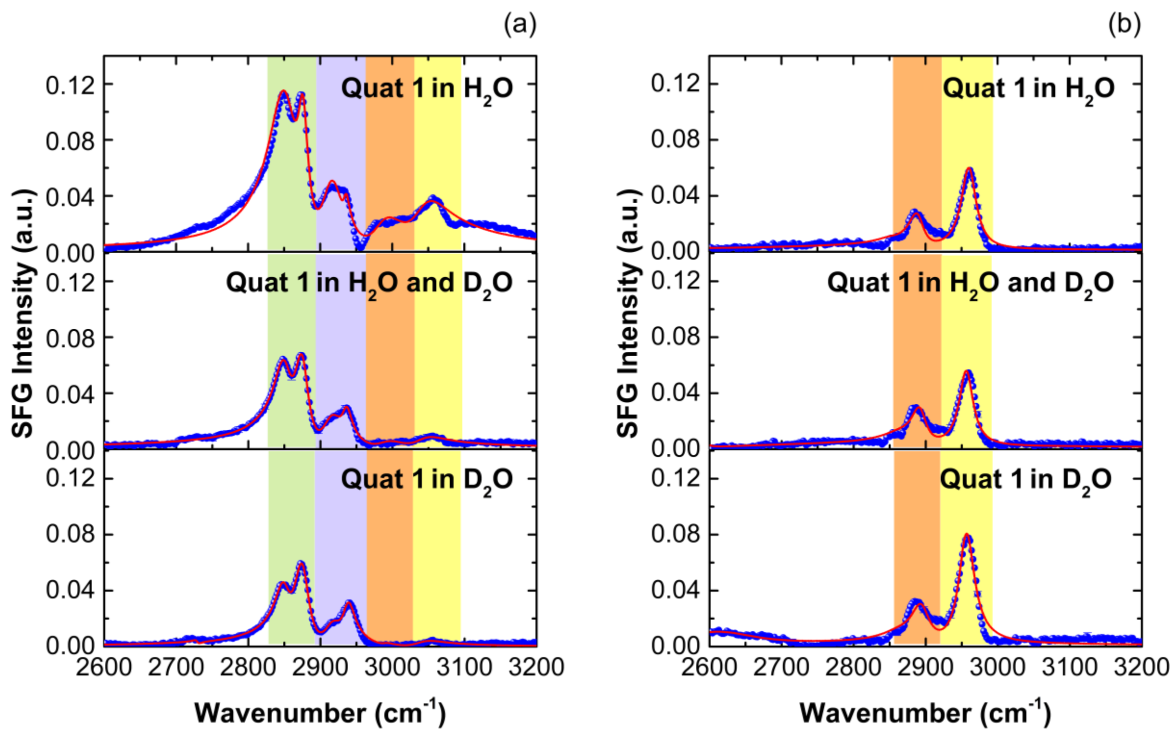

Figure 1. Fitted SFG spectra at a Quat **1** solution (8.0 mM) in H_2O, D_2O, and in a 1:1 mixture of H_2O and D_2O at (a) SSP and (b) PPP polarization combinations acquired from 2800 to 3000 cm^{-1}

(3 IR centers with a full width at half maximum (FWHM) of ~287 cm^{-1}). See narrative for color coding.

The enhancement in the N-CH_3 and aromatic vibrational modes signal from H_2O to D_2O is likely the result of a constructive interference between CH and the tail of H_2O vibrational modes. H_2O-D_2O exchange experiments reveal that the spectral shapes and peak intensities are significantly influenced by interference from OH oscillators of H_2O.[34] The constructive interference between the CH and the OH resonances creates an enhancement of the SFG intensity of the peaks, whereas as a destructive interference creates a dip in the spectrum.[9, 35] The peak enhancement in H_2O is more evident when the concentration of the surfactant is low (See Figure S3), and the intensity of the CH signal increases as the intensity of the OH vibrational mode increases. In a study carried out by Geiger and co-workers, the SFG spectra of lipid bilayers in H_2O showed a peak at ~2980 cm^{-1} that was caused by the interference between CH and OH stretches in the aqueous phase; the latter was not observed in D_2O.[34] The relative amplification of the spectral intensity of Quat **1** in H_2O compared to Quat **1** in D_2O caused by the CH/OH band interference would justify the relatively low intensity of the ~3050 cm^{-1} peak observed for Quat **1** in D_2O, as there are no OH vibrational bands that contribute to the amplification of the intensity. Geiger and co-workers also reported that CH signals from lipid bilayers are less intense in D_2O compared to H_2O.[36]

We also propose that the reduced intensity of the headgroup vibrational modes could be the result of a near zero-sum of net orientations of the N-CH_3 groups among all conformers of Quat **1** present at the interface, caused by a conformational change of the headgroup in D_2O. To support this statement, we present the SFG spectra of Quat **1** in H_2O under different ionic strengths to evaluate any interference effect caused by the OH vibrational band and/or a third-order effect introduced by the bulk water (See Figure S4 (a)). At an interface where there is an electrostatic field, a third order effect or a $\chi^{(3)}$ interaction from the bulk water can also contribute to the overall SFG intensity.[9] Geiger[36] showed that as the salt concentration is increased, the SFG intensity of the CH and OH vibrational modes is reduced, which is consistent with the changes in the combined contributions from second order resonant susceptibility ($\chi^{(2)}$) and third order optical properties of the bulk water given by the $\chi^{(3)}$ term to the overall SFG signal generation process of charged interfaces. In the absence of phase resolved measurements, the contributions of $\chi^{(3)}$ can be qualitatively estimated by determining the intensity difference between high and low salt conditions.[36] In our case, the signal from N-CH_3 SS and N-CH_3 AS modes became more apparent as the H_2O signal weakened by adding 1% (~0.17 mM) and 10% (1.7 mM) sodium chloride to the sample of interest. Now, it is more evident from the SSP spectrum at high ionic strength that the observation of the N-CH_3 vibrational modes are not solely caused by the contributions of constructive interference from the CH and OH vibrational modes and $\chi^{(3)}$ effect.

For any vibrational mode to be SFG inactive, in general, the molecules must be in a centrosymmetric environment where there is inversion symmetry (within the electric-dipole approximation).[37] Also, any of the vibrational mode coming close to an orientation parallel to the surface will result in diminishing SFG signals.[38] The absence of a particular vibrational mode could also come from the motional averaging effect of surface molecules; the SFG signal is affected if the rotational timescale for the surface molecules is comparable or faster than the vibrational dephasing time.[39-40] To test the latter possibility, we calculated the free Gibbs energy of torsion for the trimethylammonium group of surfactant **2** around its N—CH_2^{octyl} axis using density functional theory (DFT), the TPSS-D3(BJ) functional[41-43] and triple-ζ def2-TZVP basis sets. The vibrational analysis was carried out for both ground and transition states of the torsion process to extract enthalpic and entropic contributions to the mechanism. A barrier of 5.7 kcal/mol was obtained, which corresponds to a torsional isomerization rate of 4.0×10^8 s^{-1}, and a conformer half-life of 1.8 ns, using the Eyring formalism. We then estimated the vibrational dephasing lifetime (VDL) of vibrational modes using the fitting results of the molecular vibration damping coefficient, Γ; the VDL, which corresponds to 1/Γ, was found to be within the ps regime (~20 ps for N-CH_3, for example). Because the half-life of a conformer is several orders of magnitude longer than the VDL of vibrational modes (1.8 ns vs. 20 ps), we should have observed the N-CH_3 vibrational modes in both H_2O and D_2O. However, since, the N-CH_3 vibrational modes are only apparent in H_2O and almost negligible in D_2O, we propose that the disappearance of N-CH_3 vibrational modes in D_2O is caused by the peculiar net orientation of all N-CH_3 groups in the various conformers present at the interface. This does not seem to be the case in H_2O.

The changes in orientation or conformation in H_2O and D_2O must be caused by subtle differences in the solvation of the ammonium head in these two solvents. Yet identifying those differences would be highly speculative, as the enthalpy and free Gibbs energy transfer of alkyl ammonium cations from H_2O to D_2O are negligible (< 0.2 ± 0.2 kcal/mol in the case of tetraethylammonium).[44-45] The transfer of non-polar species from H_2O to D_2O is barely favorable (48 cal/mol in the case of argon at 25 ºC),[46] while the transfer of hard Lewis acids such as Ca^{2+} or Ba^{2+} is unfavorable (by 1.3 and 1.5 kcal/mol, respectively).[44] In Quat **1**, the alkyl substituents of the ammonium group reduce its electrostatic interactions with the solvent, and dampen the impact of solvent isotopic substitution on solvation. Further complicating the analysis of the solvent effect is the coexistence of multiple Quat **1** conformations with similar stabilities. DFT optimizations and vibrational analysis (see above) in conjunction with the IEFPCM continuum solvation model,[47] were used to screen the conformations. We present here the three most stable conformers (see Figure 2), with conformer **1a** and **1c** being just 0.2 and 0.8 kcal/mol less stable than conformer **1b**, respectively.

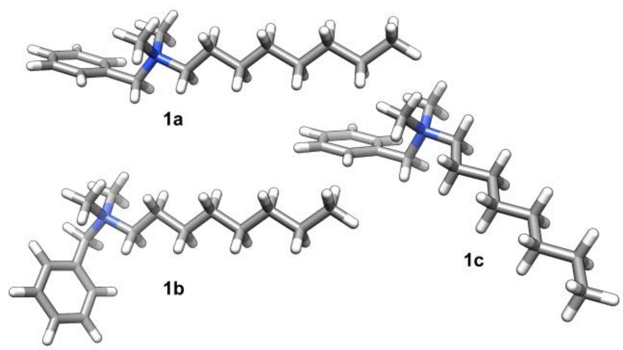

Figure 2. The three most stable conformers of Quat **1**, as determined by DFT calculations.

As a control, we recorded the SFG spectra of trimethyloctylammonium bromide (**2**; OTAB), which has an octyl hydrophobic chain and lacks the benzyl group in the headgroup (Figure S5). We observed that the vibrational modes from the headgroup are evident in H_2O and almost negligible in D_2O, similarly to Quat **1**. A peak positioned at ~3050 cm^{-1} and assigned to the N-CH_3 AS mode was observed from the SSP SFG spectrum (see Figure S6 in SI where a comparison of Quat **1** and OTAB **2** is provided), thereby confirming the presence of N-CH_3 vibrational modes at the air-water interface. Moreover, the ~3050 cm^{-1} peak observed in OTAB (**2**) in D_2O is minimal (see Figure S5 bottom panel); this suggests that the aromatic stretches could contribute to the ~3050 cm^{-1} peak observed for Quat **1** in D_2O.

An evident shift of the OH stretch tail compared to pure H_2O is observed closer to the position of the headgroup's vibrational modes (see Figures 1a and S7, ~3175 cm^{-1}), which can be attributed to an increased electrostatic field in the double-layer region as a result of the separation between the headgroup and the bromide ions as counterions.[9] The enhanced SFG signal at the lower frequency (~3175 cm^{-1}) could be caused by increased hydrogen bonding between the cationic head group and the interfacial water molecules, which then engage in further hydrogen bonding within the double-layer.[9] Also, due to the positively charged nature of the headgroup, destructive interference between the CH_3 FR and the OH stretch vibrational mode created a dip positioned at ~2954 cm^{-1}. This dip is not observed in D_2O (see Figure 1a).

Quat 1 Octyl Tail. Isotopic substitution of the solvent also affects the conformation of the tail group. The CH_2 SS (~2850 cm^{-1}) to CH_3 SS (~2875 cm^{-1}) signal ratio decreases from H_2O to D_2O (see Figure S7); this indicates a decrease in the number of gauche defects in the octyl chain and an increase in conformational order in the monolayer.[9, 38, 48] This observation indicates an improved hydrophobic interaction of the tails that may result from or even cause the conformational change of the head group in D_2O.[3]

We note that in the SSP spectra of the mixed solvent system, features of both H_2O and D_2O spectra are observed. The octyl chain conformation in the mixture of solvents is more similar to the one in H_2O, and the head group conformation is more similar to the one in D_2O.

Interactions between Quat 1 and the solvent. SFG spectra of the 1:1 H_2O/D_2O mixture, both in the absence and in the presence of Quat **1**, were collected in the O-D, C-H, and O-H vibrational regions to investigate further H_2O and D_2O interactions with the surfactant (see Figure 3). As noted above, the cationic character of Quat **1** creates an electrostatic field once adsorbed at the interface; this field then influences the orientation of the water molecules at the air-liquid interface.[27, 35] The motivation behind the 1:1 isotopic dilution is to minimize the vibrational coupling that exists in both H_2O and D_2O molecular systems. This intramolecular interaction results from the coupling of the symmetric stretch vibrations split by a Fermi resonance with the overtone of the water bending mode. This interaction gives rise to a more complicated double peak feature in the SFG spectra of aqueous interfaces.[49-51] Using the proper ratio between H_2O and D_2O in a mixed solvent system can result in the observation of the fundamental OD and OH stretch vibrational modes via decoupling of the intramolecular forces.[49-51] Also, the intramolecular coupling dominates the vibrational response from H_2O/D_2O interfaces, and the frequency of the two OH/OD stretch peaks becomes less sensitive to the fine details of the local H-bonding environment.[49] Therefore, to characterize the H_2O and D_2O interactions with the surfactant, it is more reliable to consider the changes in the HOD frequency, than only considering the spectra of Quat **1** in pure solvent systems. In our experiment, we selected 1:2:1 ratio (H_2O/HOD/D_2O) to observe subtle changes in the interactions between Quat **1** and the solvents (pure and mixed solvent systems-See Figure S7). After decoupling, The OH and OD stretch positions (see Figure 3) are indicative of the H-bonding strength of water or D_2O at the interfaces.[49, 52-55] In the OD region, in the absence of Quat **1**, the broad peak centered at ~2475 cm^{-1} is assigned to contributions of the OD stretch vibrational mode of HOD and residual D_2O (see blue curve in Figure 3).[50] The sharp peak observed at 2740 cm^{-1} is assigned to the dangling mode of free OD. In the OH region, in the absence of Quat **1**, the peak at ~3300-3450 cm^{-1} is assigned to vibrational mode contributions from HOD and residual H_2O molecules.[55] The OH stretch vibrational mode is centered at ~3340 cm^{-1} [50] while the dangling mode of free OH is observed at ~3700 cm^{-1}.[56]

As mentioned before, we varied the concentration of salt in the solution to verify and emphasize the presence of the headgroup's vibrational modes with reduced interference from the OH vibrational modes. In relation to what happens at the solvent level, the ionic strength of the solution increases, thereby the Debye screening length decreases; the volume of the non-centrosymmetric region of the interface that generates the SFG signal thus decreases as well.[57] We have provided a comparison of SFG spectra of Quat **1** from 2800 cm^{-1} to 3800 cm^{-1} (See Figure S8). We do not observe any peak shift of the OH stretch (~3175 cm^{-1}) going from 0% salt to 1% salt. This suggests the 1% salt concentration has only a minor impact on the hydrogen bonding network in the double- layer.[36] However, when the salt concentration is increased up to 10%, the peak at ~ 3175 cm^{-1} shifted to ~3250 cm^{-1} suggesting a change in the network.

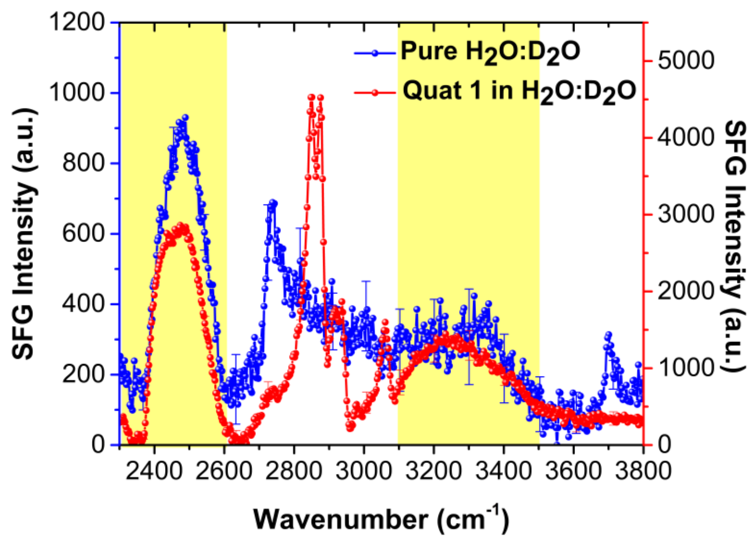

Figure 3. SFG spectra of a 1:1 mixture of H_2O and D_2O in the absence (blue curve) and presence (red curve) of Quat **1** (8.0 mM) with an SSP polarization combination. The yellow section highlights both the OD and the OH regions.

In the presence of Quat **1** (see red curve in Figure 3), the vibrational modes from free OD and free OH dangling modes (~2740 and ~3700 cm^{-1}, respectively) are not visible. This observation could be due to (1) an ordered orientation of the water molecules at the interface as influenced by the ammonium-based headgroup[27] and (2) the adsorption of more surfactant molecules at the air-water interface compared to the number of interfacial water molecules.[58] The shoulder positioned close to ~2475 cm^{-1} at approximately 2420 cm^{-1} is assigned to the bonded OD stretch of a structured configuration;[9] this spectral feature suggests a more bonded D_2O structure at the interface in the presence of the surfactant. Yet because the broad peak at 2475 cm^{-1} remains significant, D_2O molecules are not completely tetrahedrally coordinated.[9,11] A similar shoulder at ~3240 cm^{-1} in the OH vibrational region also indicates that H_2O is more ordered at the interface in the presence of the surfactant.[11]

Concentration Dependence. We then tested whether the concentration of Quat **1** would affect its arrangement at the air-liquid interface in H_2O and D_2O. Surface tension measurements and isothermal titration calorimetry (ITC) were both used to determine the critical micelle concentration (CMC; see SI section for details). Surface tensions decreased from 76.1 ± 0.1 to 44.5 ± 0.03 mN m^{-1} and from 70.0 ± 0.3 to 44.6 ± 0.1 mN m^{-1} upon addition of Quat **1** to H_2O and D_2O, respectively (up to 8.0 mM; see Figure S9 in the SI section). The surface tension measurement did not reach the CMC value for Quat **1**. Although, the surface tension values were obtained for 8 mM Quat **1** in H_2O (44.5 ± 0.03 mN m^{-1}), 1:1 H_2O:D_2O (47.5 ± 0.1 mN m^{-1}), and D_2O (44.6 ± 0.1 mN m^{-1}). In ITC experiments, aliquots of a concentrated solution of Quat **1** (0.30 M) were added to the pure solvent, and the heat generated was measured after each addition. Often abrupt changes in the enthalpograms indicate that CMC has been reached.[59-63] Using this method, CMC in D_2O was estimated at 12 mM (see Figure S10 for the enthalpogram); experiments carried out in water were inconclusive, as the recorded enthalpograms were no different from those obtained upon dilution of a solute that does not form micelles. Concentrations below and above CMC were chosen for Quat **1** to test concentration effects on the arrangement at the water (or D_2O)-air interface (0.5, 8.0 and 20 mM; see Figure S3, and Tables S4-S7). We observed the vibrational modes described above at all concentrations in both

H_2O and D_2O, as well as similar CH_2 SS to CH_3 SS ratios. The arrangement of Quat **1**, including the numbers of gauche defects in the octyl tail, is thus concentration independent.

Orientational Analysis. The mathematical details of the orientational analysis were previously reported by our group,[16-17] and the parameters used to generate the simulated SFG curves, the average tilt angles, and the orientation distribution angles of the terminal methyl group are provided in Table S8. We then determined the average orientation of the tail relative to the air-water interface using the ratio between the CH_3 SS and CH_3 AS signals in the PPP polarization combination (see Figures S11-S13 and Table S9). It has recently been reported that analyzing PPP is beneficial compared to SSP and PPP polarization combinations because one can avoid difficulties resulting from the CH_3 SS split caused by Fermi interaction with an overtone of the bending mode and interference of the CH vibrational modes with the OH stretch of the interfacial water.[27, 64] A range of 30.8 – 40.5º was found for the average tilt angle (θ) of the terminal methyl group of the alkyl tail. In an all-trans methylene configuration, the difference in tilts between methyl groups and the overall alkyl chain is 41.5º.[65-67] Therefore, the tilt for the alkyl tail would range from 1.0º to 10.8º relative to the surface normal. This supports an ordered monolayer adsorbed at the air-water interface.[10] Neither the concentration of Quat **1**, nor the nature of solvent affected the tilt angle (see Table S9).

CONCLUSION

In summary, we identified a profound isotopic effect on the geometry and arrangement of positive surfactant **1** at the air-H_2O and air-D_2O interface. Addition of D_2O rearranges its dimethylamino group parallel to the interface (on average), and straightens its octyl chain (i.e., reduces the number of its gauche defects). We also showed that the ammonium unit reinforces H_2O, HOD and D_2O cohesion at the interface.

ASSOCIATED CONTENT

Supporting Information. The Supporting Information is available free of charge on the ACS Publications website via the Internet at http://pubs.acs.org.

Supporting spectral data of NMR and SFG, fitting results, simulation parameters, and information on CMC determination. (PDF)

AUTHOR INFORMATION

Corresponding Authors:

*E-mail: cimatu@ohio.edu. Tel: +1-740-593-2308.

*E-mail: masson@ohio.edu. Tel: +1-740-593-9992.

ACKNOWLEDGMENT

This work is supported in part by a grant from the National Science Foundation (NSF; grant CBET-1705817). The authors also thank NSF (grants CHE-0947031 and CHE-1338000) for the acquisition of the femtosecond laser and nuclear magnetic spectrometer. KK and EM thank NSF (grant CHE-1507321), the American Chemical Society Petroleum Research Fund (grant 56375-ND4) and the Roenigk Foundation for their ongoing support. The authors would like to thank Drs. David Young, Srdjan Nesic, and Sumit Sharma from the Institute of Corrosion and Multiphase Technology (ICMT) in the Department of Chemical and Biomolecular Engineering at Ohio University for fruitful discussions. Additionally, the authors are grateful to multiple Ohio University entities for additional financial support (the Department of Chemistry and

Biochemistry, the College of Arts and Sciences, the Vice President for Research, the Nanoscale and Quantum Phenomena Institute, and the Condensed Matter and Surface Science program).

REFERENCES

1. Chang, N. J.; Kaler, E. W., The Structure of Sodium Dodecyl Sulfate Micelles in Solutions of Water and Deuterium Oxide. *The Journal of Physical Chemistry* **1985**, *89*, 2996-3000.
2. Bastardo, L. A.; Mészáros, R.; Varga, I.; Gilanyi, T.; Cleasson, P. M., Deuterium Isotope Effects on the Interaction between Hyperbranched Polyethylene Imine and an Anionic Surfactant. *The Journal of Physical Chemistry B* **2005**, *109*, 16196-16202.
3. Whiddon, C.; Söderman, O., Unusually Large Deuterium Isotope Effects in the Phase Diagram of a Mixed Alkylglucoside Surfactant/Water System. *Langmuir* **2001**, *17*, 1803-1806.
4. Hammouda, B.; Ho, D.; Kline, S., Sans from Poly (Ethylene Oxide)/Water Systems. *Macromolecules* **2002**, *35*, 8578-8585.
5. Petrova, T.; Dooley, R. B., Revised Release on Surface Tension of Ordinary Water Substance. *The International Association for the Properties of Water and Steam, IAPWS, Moscow, Russia* **2014**.
6. Cooper, J. R.; Dooley, R. B., IAPWS Release on Surface Tension of Heavy Water Substance. *Int. Assoc. for the Properties of Water and Steam* **1994**, 1-4.
7. Haynes, W. M., *CRC Handbook of Chemistry and Physics*; CRC press, 2014.
8. Wolfsberg, M.; Van Hook, W. A.; Paneth, P., Isotope Effects on Dipole Moments, Polarizability, NMR Shielding, and Molar Volume. In *Isotope Effects*, Springer: 2009; pp 389-412.
9. Gragson, D. E.; McCarty, B. M.; Richmond, G. L., Surfactant/Water Interactions at the Air/Water Interface Probed by Vibrational Sum Frequency Generation. *The Journal of Physical Chemistry* **1996**, *100*, 14272-14275.
10. Schleeger, M.; Nagata, Y.; Bonn, M., Quantifying Surfactant Alkyl Chain Orientation and Conformational Order from Sum Frequency Generation Spectra of CH Modes at the Surfactant–Water Interface. *The Journal of Physical Chemistry Letters* **2014**, *5*, 3737-3741.
11. Gragson, D. E.; McCarty, B. M.; Richmond, G. L., Ordering of Interfacial Water Molecules at the Charged Air/Water Interface Observed by Vibrational Sum Frequency Generation. *Journal of the American Chemical Society* **1997**, *119*, 6144-6152.
12. Mang, J. Y.; Choi, D. H.; Han, M. J. In *Comparison Studies on Nitrile-Butadiene Rubber Nanocomposites Depending on the Organically Modified Montmorillonites*, 2007; Trans Tech Publ: pp 83-86.
13. Migahed, M. A.; Al-Sabagh, A. M., Beneficial Role of Surfactants as Corrosion Inhibitors in Petroleum Industry: A Review Article. *Chemical Engineering Communications* **2009**, *196*, 1054-1075.
14. Zhu, Y.; FreeM, M. L., Effects of Surfactant Aggregation and Adsorption on Steel Corrosion Inhibition in Salt Solution. *Polymer Sciences* **2015**.
15. Conboy, J. C.; Messmer, M. C.; Richmond, G. L., Investigation of Surfactant Conformation and Order at the Liquid− Liquid Interface by Total Internal Reflection Sum-Frequency Vibrational Spectroscopy. *The Journal of Physical Chemistry* **1996**, *100*, 7617-7622.

16. Chan, S. C.; Jang, J. H.; Cimatu, K. L. A., Orientational Analysis of Interfacial Molecular Groups of 2-Methoxyethyl Methacrylate Monomer Using Femtosecond Sum Frequency Generation Spectroscopy. *The Journal of Physical Chemistry C* **2016**.
17. Premadasa, U. I.; Adhikari, N. M.; Baral, S.; Aboelenen, A. M.; Cimatu, K. L. A., Conformational Changes of Methacrylate-Based Monomers at the Air-Liquid Interface Due to Bulky Substituents. *The Journal of Physical Chemistry C* **2017**.
18. Duplan, J. C.; Mahi, L.; Brunet, J. L., NMR Determination of the Equilibrium Constant for the Liquid H_2O–D_2O Mixture. *Chemical Physics Letters* **2005**, *413*, 400-403.
19. Quast, A. D.; Wilde, N. C.; Matthews, S. S.; Maughan, S. T.; Castle, S. L.; Patterson, J. E., Improved Assignment of Vibrational Modes in Sum-Frequency Spectra in the C H Stretch Region for Surface-Bound C 18 Alkylsilanes. *Vibrational Spectroscopy* **2012**, *61*, 17-24.
20. Richter, L. J.; Petralli-Mallow, T. P.; Stephenson, J. C., Vibrationally Resolved Sum-Frequency Generation with Broad-Bandwidth Infrared Pulses. *Optics Letters* **1998**, *23*, 1594-1596.
21. Verreault, D.; Kurz, V.; Howell, C.; Koelsch, P., Sample Cells for Probing Solid/Liquid Interfaces with Broadband Sum Frequency Generation Spectroscopy. *Review of Scientific Instruments* **2010**, *81*, 063111.
22. Bain, C. D.; Davies, P. B.; Ong, T. H.; Ward, R. N.; Brown, M. A., Quantitative Analysis of Monolayer Composition by Sum Frequency Vibrational Spectroscopy. *Langmuir* **1991**, *7*, 1563-1566.
23. Ma, G.; Allen, H. C., Surface Studies of Aqueous Methanol Solutions by Vibrational Broad Bandwidth Sum Frequency Generation Spectroscopy. *The Journal of Physical Chemistry B* **2003**, *107*, 6343-6349.
24. Ishiyama, T.; Sokolov, V. V.; Morita, A., Molecular Dynamics Simulation of Liquid Methanol. I. Molecular Modeling Including C–H Vibration and Fermi Resonance. *The Journal of Chemical Physics* **2011**, *134*, 024509.
25. Tyrode, E.; Rutland, M. W.; Bain, C. D., Adsorption of CTAB on Hydrophilic Silica Studied by Linear and Nonlinear Optical Spectroscopy. *Journal of the American Chemical Society* **2008**, *130*, 17434-17445.
26. O'Leary, T. J.; Levin, I. W., Raman Spectroscopic Study of the Melting Behavior of Anhydrous Dipalmitoylphosphatidylcholine Bilayers. *The Journal of Physical Chemistry* **1984**, *88*, 1790-1796.
27. Nguyen, K. T.; Nguyen, A. V.; Evans, G. M., Interfacial Water Structure at Surfactant Concentrations Below and Above the Critical Micelle Concentration as Revealed by Sum Frequency Generation Vibrational Spectroscopy. *The Journal of Physical Chemistry C* **2015**, *119*, 15477-15481.
28. Chen, C.-Y.; Even, M. A.; Wang, J.; Chen, Z., Sum Frequency Generation Vibrational Spectroscopy Studies on Molecular Conformation of Liquid Polymers Poly (Ethylene Glycol) and Poly (Propylene Glycol) at Different Interfaces. *Macromolecules* **2002**, *35*, 9130-9135.
29. Hommel, E. L.; Allen, H. C., The Air–Liquid Interface of Benzene, Toluene, M-Xylene, and Mesitylene: A Sum Frequency, Raman, and Infrared Spectroscopic Study. *Analyst* **2003**, *128*, 750-755.
30. Bzeih, W.; Gheribi, A.; Wood-Adams, P. M.; Hayes, P. L., Dependence of the Surface Structure of Polystyrene on Chain Molecular Weight Investigated by Sum Frequency Generation Spectroscopy. *The Journal of Physical Chemistry C* **2018**, *122*, 3838-3845.

31. Feng, R. J.; Li, X.; Zhang, Z.; Lu, Z.; Guo, Y., Spectral Assignment and Orientational Analysis in a Vibrational Sum Frequency Generation Study of DPPC Monolayers at the Air/Water Interface. *Journal of Chemical Physics* **2016**, *145*.
32. Ishiyama, T.; Sokolov, V. V.; Morita, A., Molecular Dynamics Simulation of Liquid Methanol. II. Unified Assignment of Infrared, Raman, and Sum Frequency Generation Vibrational Spectra in Methyl C–H Stretching Region. *The Journal of Chemical Physics* **2011**, *134*, 024510.
33. Goussous, S. A.; Casford, M. T. L.; Johnson, S. A.; Davies, P. B., A Structural and Temporal Study of the Surfactants Behenyltrimethylammonium Methosulfate and Behenyltrimethylammonium Chloride Adsorbed at Air/Water and Air/Glass Interfaces Using Sum Frequency Generation Spectroscopy. *Journal of Colloid and Interface Science* **2017**, *488*, 365-372.
34. Olenick, L. L.; Chase, H. M.; Fu, L.; Zhang, Y.; McGeachy, A. C.; Dogangun, M.; Walter, S. R.; Wang, H.-F.; Geiger, F. M., Single-Component Supported Lipid Bilayers Probed Using Broadband Nonlinear Optics. *Physical Chemistry Chemical Physics* **2018**, 20, 3063-3072.
35. Nihonyanagi, S.; Yamaguchi, S.; Tahara, T., Direct Evidence for Orientational Flip-Flop of Water Molecules at Charged Interfaces: A Heterodyne-Detected Vibrational Sum Frequency Generation Study. *The Journal of Chemical Physics* **2009**, *130*, 204704.
36. Dogangun, M.; Ohno, P. E.; Liang, D.; McGeachy, A. C.; Be, A. G.; Dalchand, N.; Li, T.; Cui, Q.; Geiger, F. M., Hydrogen-Bond Networks near Supported Lipid Bilayers from Vibrational Sum Frequency Generation Experiments and Atomistic Simulations. *The Journal of Physical Chemistry B* **2018**, 122 (18), pp 4870–4879.
37. Johnson, C. M.; Tyrode, E., Study of the Adsorption of Sodium Dodecyl Sulfate (SDS) at the Air/Water Interface: Targeting the Sulfate Headgroup Using Vibrational Sum Frequency Spectroscopy. *Physical Chemistry Chemical Physics* **2005**, *7*, 2635-2640.
38. Lambert, A. G.; Davies, P. B.; Neivandt, D. J., Implementing the Theory of Sum Frequency Generation Vibrational Spectroscopy: A Tutorial Review. *Applied Spectroscopy Reviews* **2005**, *40*, 103-145.
39. Wei, X.; Shen, Y. R., Motional Effect in Surface Sum-Frequency Vibrational Spectroscopy. *Physical Review Letters* **2001**, *86*, 4799.
40. Sung, J.; Kim, D., Motional Effect on the Sum-Frequency Vibrational Spectra from Methanol Surface. *Journal Korean Physical Society* **2007**, *51*, 145.
41. Grimme, S.; Ehrlich, S.; Goerigk, L., Effect of the Damping Function in Dispersion Corrected Density Functional Theory. *Journal of Computational Chemistry* **2011**, *32*, 1456-1465.
42. Tao, J.; Perdew, J. P.; Staroverov, V. N.; Scuseria, G. E., Climbing the Density Functional Ladder: Nonempirical Meta–Generalized Gradient Approximation Designed for Molecules and Solids. *Physical Review Letters* **2003**, *91*, 146401.
43. Grimme, S.; Antony, J.; Ehrlich, S.; Krieg, H., A Consistent and Accurate Ab Initio Parametrization of Density Functional Dispersion Correction (DFT-D) for the 94 Elements H-Pu. *The Journal of Chemical Physics* **2010**, *132*, 154104.
44. Rekharsky, M. V.; Inoue, Y., Solvent and Guest Isotope Effects on Complexation Thermodynamics of A-, B-, and 6-Amino-6-Deoxy-B-Cyclodextrins. *Journal of the American Chemical Society* **2002**, *124*, 12361-12371.
45. Marcus, Y., Ion Solvation John Wiley. Chichester: 1985.

46. Graziano, G., On the Solvent Isotope Effect in Hydrophobic Hydration. *The Journal of Physical Chemistry B* **2000**, *104*, 9249-9254.
47. Tomasi, J.; Mennucci, B.; Cammi, R., Quantum Mechanical Continuum Solvation Models. *Chemical Reviews* **2005**, *105*, 2999-3094.
48. Ge, A. M.; Peng, Q. L.; Qiao, L.; Yepuri, N. R.; Darwish, T. A.; Matsusaki, M.; Akashi, M.; Ye, S., Molecular Orientation of Organic Thin Films on Dielectric Solid Substrates: A Phase-Sensitive Vibrational SFG Study. *Physical Chemistry Chemical Physics* **2015**, *17*, 18072-18078.
49. Sovago, M.; Campen, R. K.; Wurpel, G. W. H.; Müller, M.; Bakker, H. J.; Bonn, M., Vibrational Response of Hydrogen-Bonded Interfacial Water Is Dominated by Intramolecular Coupling. *Physical Review Letters* **2008**, *100*, 173901.
50. Sovago, M.; Campen, R. K.; Bakker, H. J.; Bonn, M., Hydrogen Bonding Strength of Interfacial Water Determined with Surface Sum Frequency Generation. *Chemical Physics Letters* **2009**, *470*, 7-12.
51. Bonn, M.; Bakker, H. J.; Tong, Y.; Backus, E. H. G., No Ice-Like Water at Aqueous Biological Interfaces. *Biointerphases* **2012**, *7*, 20.
52. Nihonyanagi, S.; Yamaguchi, S.; Tahara, T., Counterion Effect on Interfacial Water at Charged Interfaces and Its Relevance to the Hofmeister Series. *Journal of the American Chemical Society* **2014**, *136*, 6155-6158.
53. Nihonyanagi, S.; Yamaguchi, S.; Tahara, T., Water Hydrogen Bond Structure near Highly Charged Interfaces Is Not Like Ice. *Journal of the American Chemical Society* **2010**, *132*, 6867-6869.
54. Nihonyanagi, S.; Ishiyama, T.; Lee, T.-k.; Yamaguchi, S.; Bonn, M.; Morita, A.; Tahara, T., Unified Molecular View of the Air/Water Interface Based on Experimental and Theoretical X(2) Spectra of an Isotopically Diluted Water Surface. *Journal of the American Chemical Society* **2011**, *133*, 16875-16880.
55. Tian, C.-S.; Shen, Y. R., Isotopic Dilution Study of the Water/Vapor Interface by Phase-Sensitive Sum Frequency Vibrational Spectroscopy. *Journal of the American Chemical Society* **2009**, *131*, 2790-2791.
56. Johnson, C. M.; Tyrode, E.; Baldelli, S.; Rutland, M. W.; Leygraf, C., A Vibrational Sum Frequency Spectroscopy Study of the Liquid−Gas Interface of Acetic Acid−Water Mixtures: 1. Surface Speciation. *The Journal of Physical Chemistry B* **2005**, *109*, 321-328.
57. Jena, K. C.; Hore, D. K., Variation of Ionic Strength Reveals the Interfacial Water Structure at a Charged Mineral Surface. *The Journal of Physical Chemistry C* **2009**, *113*, 15364-15372.
58. Livingstone, R. A.; Nagata, Y.; Bonn, M.; Backus, E. H. G., Two Types of Water at the Water–Surfactant Interface Revealed by Time-Resolved Vibrational Spectroscopy. *Journal of the American Chemical Society* **2015**, *137*, 14912-14919.
59. Bouchemal, K.; Agnely, F.; Koffi, A.; Ponchel, G., A Concise Analysis of the Effect of Temperature and Propanediol-1, 2 on Pluronic F127 Micellization Using Isothermal Titration Microcalorimetry. *Journal of Colloid and Interface Science* **2009**, *338*, 169-176.
60. Kamboj, R.; Bharmoria, P.; Chauhan, V.; Singh, G.; Kumar, A.; Singh, S.; Kang, T. S., Effect of Cationic Head Group on Micellization Behavior of New Amide-Functionalized Surface Active Ionic Liquids. *Physical Chemistry Chemical Physics* **2014**, *16*, 26040-26050.

61. Li, Y.; Xu, R.; Couderc, S.; Bloor, M.; Wyn-Jones, E.; Holzwarth, J. F., Binding of Sodium Dodecyl Sulfate (SDS) to the ABA Block Copolymer Pluronic F127 (EO97PO69EO97): F127 Aggregation Induced by SDS. *Langmuir* **2001**, *17*, 183-188.
62. Rao, K. S.; Gehlot, P. S.; Gupta, H.; Drechsler, M.; Kumar, A., Sodium Bromide Induced Micelle to Vesicle Transitions of Newly Synthesized Anionic Surface Active Ionic Liquids Based on Dodecylbenzenesulfonate. *The Journal of Physical Chemistry B* **2015**, *119*, 4263-4274.
63. Lah, J.; Pohar, C.; Vesnaver, G., Calorimetric Study of the Micellization of Alkylpyridinium and Alkyltrimethylammonium Bromides in Water. *The Journal of Physical Chemistry B* **2000**, *104*, 2522-2526.
64. Saha, A.; SenGupta, S.; Kumar, A.; Naik, P. D., Interaction of Sodium Dodecyl Sulfate with Lipid Monolayer Studied by Sum Frequency Generation Spectroscopy at Air–Water Interface. *The Journal of Physical Chemistry C* **2017**, *121*, 13175-13182.
65. Ma, G.; Allen, H. C., Dppc Langmuir Monolayer at the Air− Water Interface: Probing the Tail and Head Groups by Vibrational Sum Frequency Generation Spectroscopy. *Langmuir* **2006**, *22*, 5341-5349.
66. Ma, G.; Allen, H. C., Condensing Effect of Palmitic Acid on DPPC in Mixed Langmuir Monolayers. *Langmuir* **2007**, *23*, 589-597.
67. Ye, S.; Noda, H.; Nishida, T.; Morita, S.; Osawa, M., Cd^{2+}-Induced Interfacial Structural Changes of Langmuir− Blodgett Films of Stearic Acid on Solid Substrates: A Sum Frequency Generation Study. *Langmuir* **2004**, *20*, 357-365.

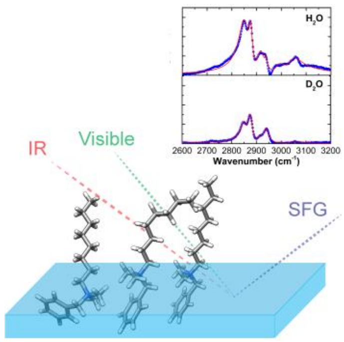
H2O
D2O
2600 2700 2800 2900 3000 3100 3200
Wavenumber (cm-1)
IR
Visible
SFG